ELSEVIER
Wear 261 (2006) 513–519
WEAR
www.elsevier.com/locate/wear

Adhesive wear behavior of $Al_xCoCrCuFeNi$ high-entropy alloys as a function of aluminum content

Jien-Min Wu [a], Su-Jien Lin [a], Jien-Wei Yeh [a,*], Swe-Kai Chen [b], Yuan-Sheng Huang [a,c], Hung-Cheng Chen [d]

[a] *Department of Materials Science and Engineering, National Tsing Hua University, Hsinchu 300, Taiwan*
[b] *Materials Science Center, National Tsing Hua University, Hsinchu 300, Taiwan*
[c] *Department of Mechanical and Electronic Engineering, Shaoguan University, Shaoguan City, Guangdong 512005, China*
[d] *Materials Research Laboratory, Industrial Technology Research Institute, Chutung 310, Taiwan*

Received 7 June 2005; received in revised form 31 October 2005; accepted 12 December 2005
Available online 19 January 2006

Abstract

The $Al_xCoCrCuFeNi$ alloys with different aluminum contents prepared by arc melting were investigated on their adhesive wear behaviors. With increasing aluminum content, both the volume fraction of BCC phase and the hardness value increase, and thus the wear coefficient decreases. Moreover, the wear mechanism changes from delamination wear to oxidative wear. For low aluminum content, $x = 0.5$, the microstructure is of simple ductile FCC phase and the worn surface is deeply grooved and undergoes a periodic delamination which produces big debris. For medium aluminum content, $x = 1.0$, the microstructure is a mixture of FCC and BCC phases, and the worn surface is deeply grooved in FCC region but smooth in BCC region. Delamination wear is still dominant although oxidative wear occurs in the smooth region. For high aluminum content, $x = 2.0$, the microstructure is of BCC phase and the worn surface is smooth and yields fine debris with high oxygen content. The high aluminum content gives a large improvement in wear resistance. This improvement is attributed to its high hardness, which not only resists plastic deformation and delamination, but also brings about the oxidative wear in which oxide film could assist the wear resistance.

Keywords: High-entropy alloy; Adhesive wear; Wear coefficient; Friction

1. Introduction

In recent years, an entirely new alloy field, high-entropy alloys with multiple principal elements in equimolar or near-equimolar ratios, has been explored by Jien-Wei Yeh et al. [1,2]. High-entropy alloys may contain at least five principal elements with the concentration of each element being between 35 and 5 at.%. Solid solutions with multi-principal elements will tend to be more stable at elevated temperatures because of their large mixing entropies [1]. The previous studies [1–6] have shown that high-entropy alloys might possess simple crystal structures, ease of nanoprecipitation, and promising properties in high hardness and superior resistance to temper softening, wear, oxidation and corrosion. Among these, $Al_xCoCrCuFeNi$ alloys have a gradual change from FCC phases to BCC phases, and hardness increase from 120 to 650 HV with increasing aluminum content. They are promising for the applications in structural and tool industries [5,6].

The wear performance of the alloys based on one principal element has been investigated widely. One of the most common forms of the coefficient of friction curves in adhesive wear test is characterized by an initial rise in the coefficient of friction, up to a peak value, followed by gradual decline to a steady-state value [7–13]. Fig. 1 shows a schematic diagram of this typical coefficient of friction versus sliding distance curve [13]. The factors influencing the friction curve of metallic materials include hardness, plastic deformation, work-hardening and evolution of crystallographic texture all of which can take place during the wear process [13,14]. Due to the importance of wear behavior of high-entropy alloys for their industrial applications, the adhesive wear behavior of $Al_xCoCrCuFeNi$ alloys is investigated in this paper.

* Corresponding author. Tel.: +886 3 5719558; fax: +886 3 5722366.
E-mail address: jwyeh@mx.nthu.edu.tw (J.-W. Yeh).

0043-1648/$ – see front matter © 2005 Elsevier B.V. All rights reserved.
doi:10.1016/j.wear.2005.12.008

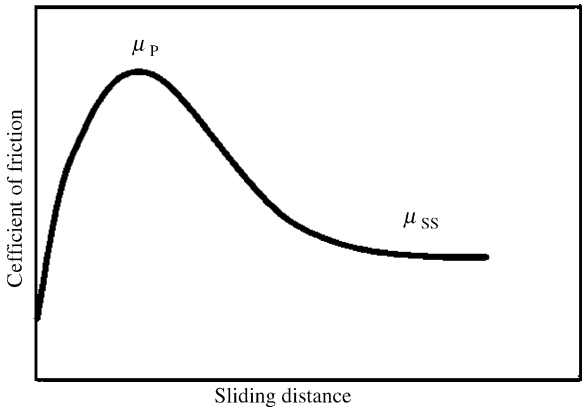

Fig. 1. Schematic diagram showing a typical coefficient of friction as a function of sliding distance. The friction curve increases rapidly to a peak value (μ_p) followed by a gradual decrease to a steady-state value (μ_{ss}).

2. Experimental details

The $Al_xCoCrCuFeNi$ high-entropy alloys with different aluminum contents ($x = 0$–2.0 in molar ratio) were prepared in this study by arc melting and casting method. The method followed the same procedure as described in reference [3]. The alloy specimens were polished and etched with *aqua regia* (HNO_3:HCl = 1:3) for observation under an optical microscope and scanning electron microscope (SEM, JEOL JSM-5410). The chemical compositions of different phases were analyzed by SEM energy dispersive spectrometry (EDS). Hardness measurements were conducted using a Vickers hardness tester (Matsuzawa Seiki MV-1) under a load of 49 N and at a loading speed of 70 μm/s for 20 s. Scattering errors were within 3%. The adhesive wear behavior of the alloys was investigated by pin-on-disk sliding using a self-made wear testing machine under dry sliding conditions as shown in Fig. 2. Pins of 8 mm diameter and 25 mm height were worn for a pre-determined distance against a 75 cm diameter disk made of SKH-51 steel with a hardness of 890 HV, at a distance of 20 mm from center, sliding speed of 0.5 m/s and normal load of 29.4 N. The sliding distance for low and medium aluminum contents, i.e. $x = 0.5$ and 1.0, was 5400 m due to their high wear loss, whereas that for high aluminum content, i.e. $x = 2.0$, was 64,800 m due to its excellent wear resistance. Both pins and counterface were polished to 0.25 μm finish before each test. Wear debris and worn surfaces were characterized using SEM and EDS. An X-ray diffractometer (XRD, Rigaku ME510-FM2, Tokyo, Japan) was used for the phase identification with the 2θ scan ranging from 20° to 100° at a speed of $1^\circ\ min^{-1}$. The typical radiation condition was 30 kV and 20 mA with a copper target. Wear coefficient is defined as follows:

$$W_r = \frac{\Delta V}{F \int_0^{L_p} \mu d_L}$$

where W_r is the wear coefficient, ΔV the volumetric loss of the specimen (pin) after sliding for a distance L_p and obtained by dividing the weight loss of the specimen after sliding by its density, μ the coefficient of friction, L the sliding distance and F is the load.

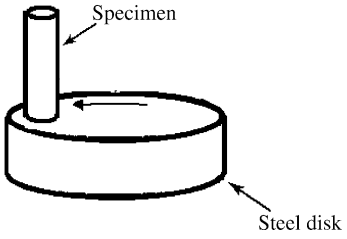

Fig. 2. Schematic drawing of wear test.

Table 1
Chemical compositions of cast $Al_xCoCrCuFeNi$ alloys in atomic percentage

x-Value	Al	Co	Cr	Cu	Fe	Ni
0.5						
Nominal	9.09	18.18	18.18	18.18	18.18	18.18
DR (BCC)	5.5	21.2	23.9	9.4	22.7	17.2
ID (Cu-rich)	12.5	5.5	4.0	59.2	5.2	13.6
1.0						
Nominal	16.67	16.67	16.67	16.67	16.67	16.67
DR (BCC)	25.5	16.1	17.2	7.4	14.6	19.2
ID (FCC + BCC)	13.0	17.3	18.3	17.5	20.0	13.9
ID (Cu-rich)	13.3	6.2	4.9	56.9	6.4	12.3
2.0						
Nominal	28.56	14.28	14.28	14.28	14.28	14.28
DR (BCC)	31.5	16.8	10.8	9.1	15.0	16.9
ID (Cu-rich)	15.1	3.4	4.2	68.2	4.0	5.1

DR, dendrite; ID, inter-dendrite.

3. Results and discussion

3.1. Microstructure and hardness of as-cast $Al_xCoCrCuFeNi$ alloys

In order to compare with the microstructure of the worn surface after adhesive wear test, the microstructure of as-cast $Al_xCoCrCuFeNi$ alloys was investigated first. Fig. 3 gives the typical microstructures of the alloys with different aluminum contents. Typical cast dendrite and interdendrite structures (defined as DR and ID in the figures, respectively) are observed in the alloys. The chemical compositions of the alloys analyzed by EDS are summarized in Table 1. Copper segregation is obviously seen in the interdendrite region. Fig. 4 shows the XRD analysis of crystal structure. It reveals that they consist of simple phases, FCC and BCC in the as-cast state. Thus for low aluminum content ($x = 0.5$), both the dendrite and Cu-rich interdendrite are of one simple FCC phase. As the aluminum content increases to $x = 1.0$, the dendrite region is of BCC phase and featured by the modulated structures of spinodal decomposition (defined as SD), while most region of the interdendrite is composed of FCC and BCC phases, and small region is the Cu-rich FCC phase. For high aluminum content ($x = 2.0$), the BCC dendrite is of spinodal structure and the small interdendrite is the Cu-rich FCC phase. It is clear that with the aluminum content increase, the volume fraction of BCC phase increases while the amount of interdendrite decreases. All these observations are in accordance with the microstructure analysis of $Al_xCoCrCuFeNi$

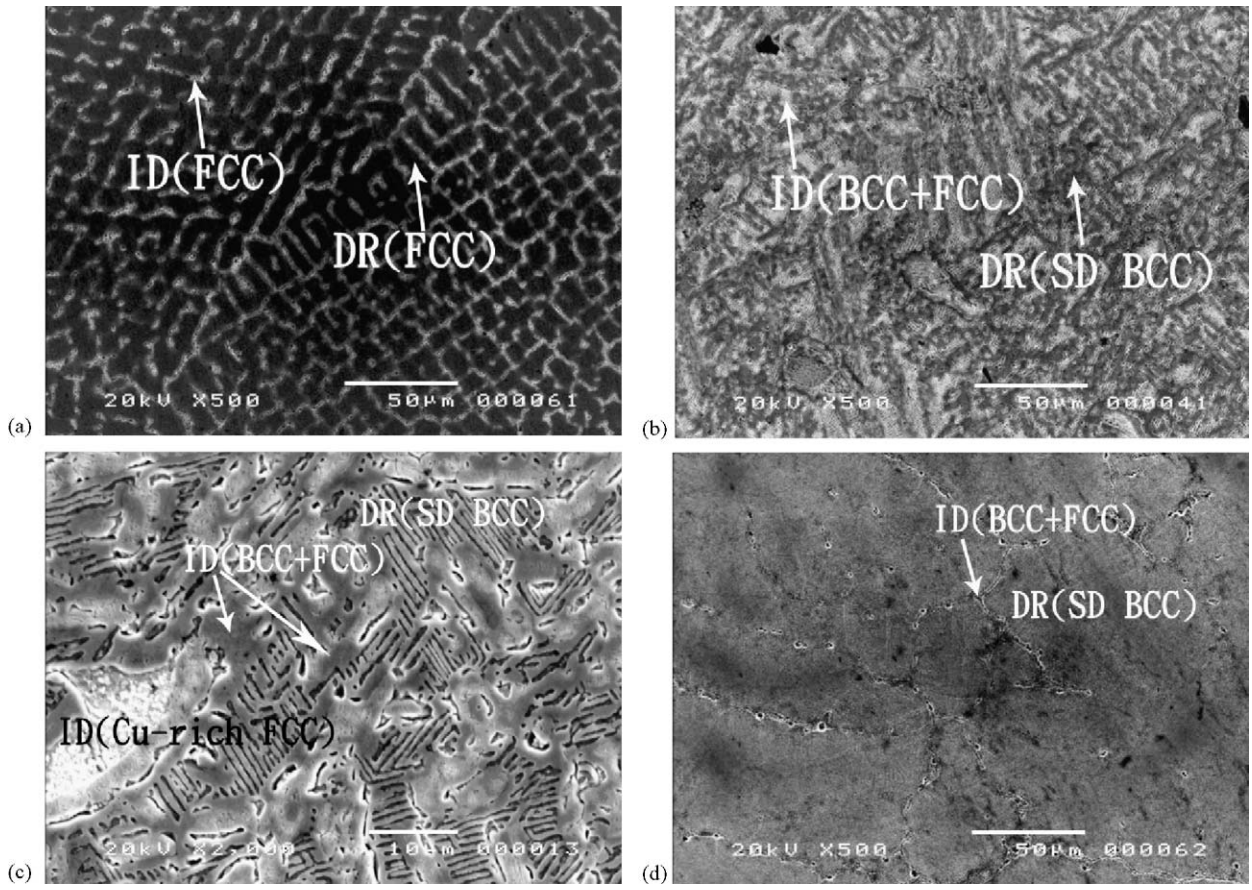

Fig. 3. SEM microstructures of as-cast $Al_xCoCrCuFeNi$ alloys with different aluminum contents (x-value): (a) 0.5; (b) 1.0; (c) 1.0; (d) 2.0 (DR: dendrite, ID: inter-dendrite, SD: spinodal decomposition).

alloys reported by Tong et al. [5] in which aluminum content varied from 0 to 3.0.

Fig. 5 shows the hardness variation with aluminum content. The hardness value rises as the aluminum content increases. In comparison with the microstructural evolution indicated in Fig. 5, it can be seen that the hardness value rise is coincident with the large increase in the volume fraction of BCC phase. This obviously implies that the BCC phase is much stronger than FCC phase by about three folds. This can be explained with three viewpoints. The first is that slip along the closest packing planes $\{1\,1\,0\}$ in BCC structure is more difficult than that along those $\{1\,1\,1\}$ in FCC structure as $\{1\,1\,0\}$ planes are less dense and more irregular and thus possess a smaller interplanar spacing and higher lattice friction for dislocation motion than $\{1\,1\,1\}$ planes in the atomic scale [15–17]. The second is due to the incorporation of stronger binding elements like Al and high melting point elements like Cr in BCC phase to increase

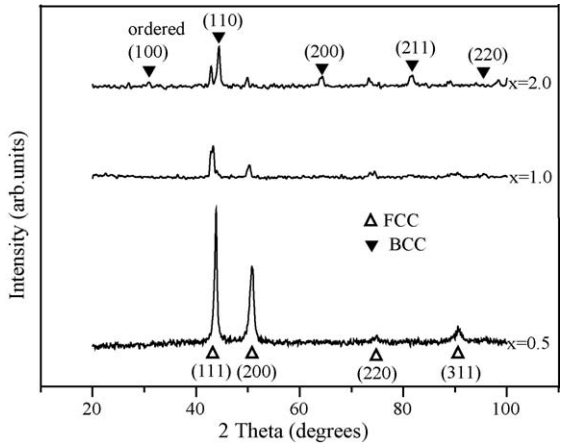

Fig. 4. XRD analyses of $Al_xCoCrCuFeNi$ alloys with different aluminum contents.

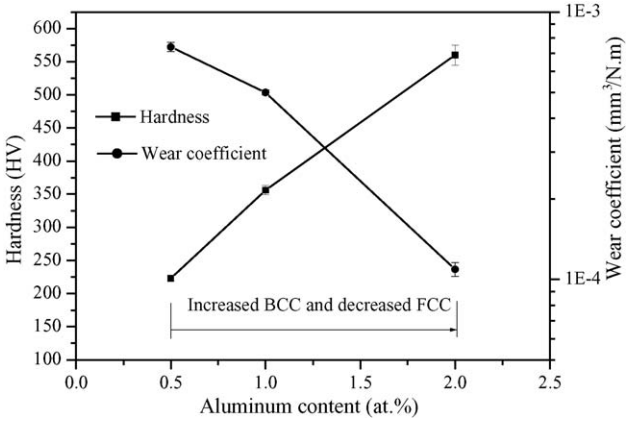

Fig. 5. Vickers hardness and wear coefficient of $Al_xCoCrCuFeNi$ alloys with different aluminum contents.

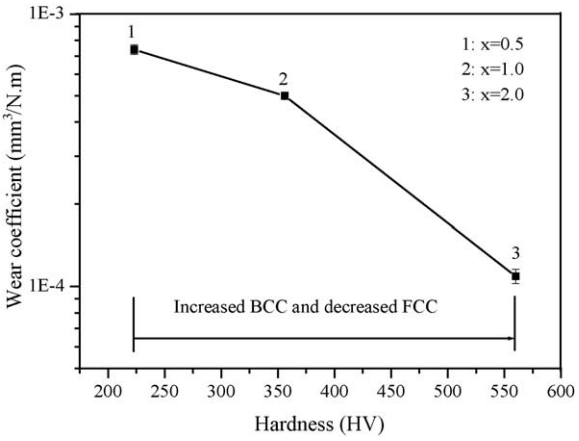

Fig. 6. Wear coefficient vs. hardness of $Al_xCoCrCuFeNi$ alloys.

the Young's modulus and the slip resistance [16,17]. The third is the spinodal decomposition of BCC phase by which a nano-spaced spinodal structure may also provide a nano-composite strengthening effect [18].

3.2. Adhesive wear behavior

3.2.1. Wear coefficient

The wear coefficient is used as a parameter to evaluate the adhesive wear resistance. Smaller wear coefficient means higher wear resistance since it requires more energy to remove the same volume. The effect of aluminum content on the wear coefficient of $Al_xCoCrCuFeNi$ alloys is shown in Fig. 5. The wear coefficient decreases as the aluminum content increases. The wear coefficient of high aluminum content is about one seventh of that of low aluminum content. Fig. 6 shows the correlation between wear coefficient and hardness. It can be seen that the wear coefficient of $Al_xCoCrCuFeNi$ alloys is sensitively related to their hardness in transition from FCC phase to BCC phase. This result is in agreement with Khruschov's conclusion, that is, the wear resistance of materials is in general proportional to their Vickers' hardness [19]. As discussed earlier, BCC phase is much stronger than FCC phase. It is reasonable that wear resistance becomes better with increasing amount of BCC phase. However, more detailed investigation as follows is required to understand the full mechanism.

3.2.2. Worn surface and debris

Fig. 7 shows the morphologies of the worn surface after test and the debris produced during this test. Obvious differences in wear surface morphology are seen as a function of aluminum content. With increasing aluminum content, surface roughness and the degree of deformation decrease. For $x = 0.5$, the worn surface is grooved and significant ductile deformation along the groove is seen. Moreover, a few lateral cracks exist in the worn surface. Compared with the debris of the $Al_{1.0}CoCrCuFeNi$ and $Al_{2.0}CoCrCuFeNi$ alloys, $Al_{0.5}CoCrCuFeNi$ alloy debris is the biggest, around 150–300 μm, and has a disk-like shape. This indicates the adhesive wear mechanism of $Al_{0.5}CoCrCuFeNi$ is predominantly of delamination wear, by which the worn surface undergoes a periodic delamination fracture [20]. This is reasonable since delamination wear is a typical mechanism for ductile metals and $Al_{0.5}CoCrCuFeNi$ alloy is composed of ductile FCC phases. The chemical composition of both the worn surface and wear debris are shown in Table 2. It can be seen that they all contain significant amount of oxygen indicating oxidation occurs on the worn surface heated by friction and deformation.

Table 2
Chemical compositions of worn surface and wear debris of $Al_xCoCrCuFeNi$ alloys in atomic percentage

x-Value	Al	Co	Cr	Cu	Fe	Ni	O
0.5							
Nominal	9.09	18.18	18.18	18.18	18.18	18.18	
Worn surface	7.2	16.5	17.3	14.7	17.5	16.2	12.4
Wear debris	6.1	16.4	16.1	15.5	16.5	15.3	16.2
1.0							
Nominal	16.67	16.67	16.67	16.67	16.67	16.67	
Worn surface	15.6	13.6	15.7	14.6	13.5	14.5	14.8
Wear debris	13.2	15.3	16.0	14.6	14.3	13.6	18.4
2.0							
Nominal	28.56	14.28	14.28	14.28	14.28	14.28	
Worn surface-A	25.1	15.9	14.2	9.1	14.9	14.1	5.6
Worn surface-B	19.4	7.7	6.7	39.8	7.7	9.6	9.2
Wear debris	12.4	6.0	5.5	6.2	6.6	6.0	56.8

For $Al_{1.0}CoCrCuFeNi$ alloy, the surface is locally grooved, but is smooth in other regions. A few lateral cracks are also observed in the worn surface. The debris size is around 80–200 μm, smaller than that of $Al_{0.5}CoCrCuFeNi$ alloy. The oxygen contents worn surface and debris are all higher than that of $Al_{0.5}CoCrCuFeNi$ alloy as shown in Table 2. This indicates that the wear type of $Al_{1.0}CoCrCuFeNi$ alloy is still predominantly of delamination wear although oxidative wear become pronounced. This is due to the fact that there is a significant portion of soft and ductile FCC phase.

In comparison with the alloys with low and medium aluminum content ($x = 0.5$ and 1.0), an increase in aluminum content to 2.0 results in a smoother worn surface, Fig. 7e, with fewer shallow abrasive grooves. Wear debris is particle-like and finer, around 10 μm in size. The percentage of oxygen on the worn surface of $Al_{2.0}CoCrCuFeNi$ alloy is lower than that of both $Al_{0.5}CoCrCuFeNi$ and $Al_{1.0}CoCrCuFeNi$, nevertheless, the oxygen concentration of wear debris is much more than that of both the $Al_{0.5}CoCrCuFeNi$ and $Al_{1.0}CoCrCuFeNi$ alloys. All these indicate that the wear mechanism is predominantly of oxidative wear. This is reasonable since the strong resistance of hard BCC phase to plastic deformation and delamination might keep the oxide layer to withstand the abrasion. Based on this, the large improvement of wear resistance in the alloy of high aluminum content is contributed by the oxide film in addition to the hardness which resists plastic deformation and delamination.

3.2.3. Coefficient of friction

Fig. 8 shows the friction coefficient for the $Al_xCoCrCuFeNi$ alloys with different aluminum contents. The coefficient of friction curves are typically characterized by two friction regimes as reported in literature [7–13]. Initially, the coefficient of fric-

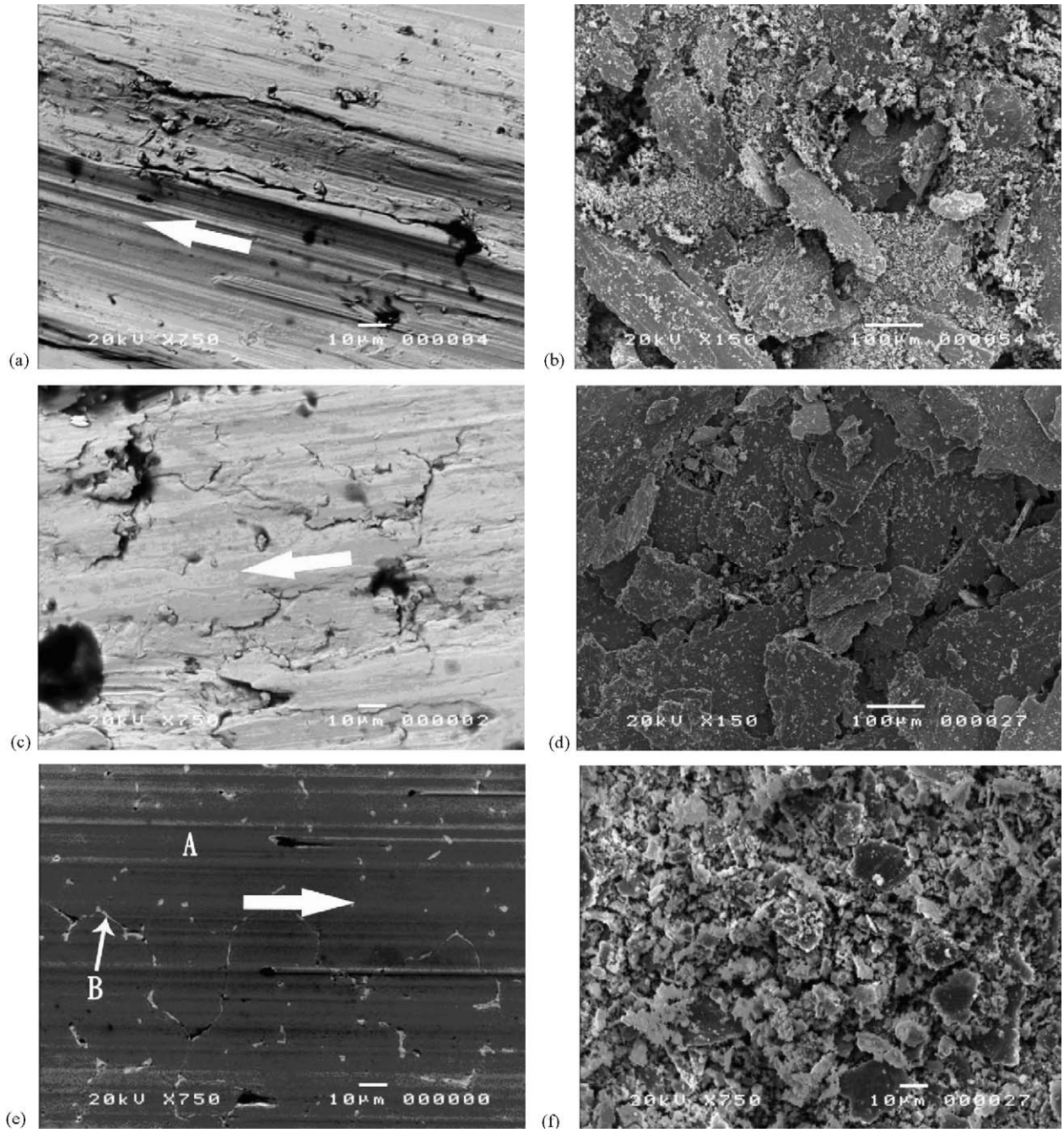

Fig. 7. SEM microstructures of worn surface and wear debris of $Al_xCoCrCuFeNi$ alloys with different aluminum contents (x-value): (a) 0.5, worn surface; (b) 0.5, debris; (c) 1.0, worn surface; (d) 1.0, debris; (e) 2.0, worn surface; (f) 2.0, debris.

tion increases rapidly until reaching a peak value μ_p. Then a gradual decrease is followed to a steady-state value μ_{ss}. It is obvious that their ranges of friction coefficient are different as listed in Table 3. Both the friction curves of $Al_{0.5}CoCrCuFeNi$ and $Al_{1.0}CoCrCuFeNi$ alloys show a peak coefficient of friction of around 0.65 and the steady value around 0.48 whereas $Al_{2.0}CoCrCuFeNi$ alloy show the range between 0.70 and 0.32. The larger peak coefficient of friction of $Al_{2.0}CoCrCuFeNi$ alloy is attributable to the fact that $Al_{2.0}CoCrCuFeNi$ alloy with high hardness (560 HV) can scratch the disk made of SKH-51 steel with a hardness of 890 HV. The smallest attainable fric-

Table 3
Summary of results on friction properties of alloys tested

Alloy	μ_p	μ_s	$\Delta\mu$
$Al_{0.5}CoCrCuFeNi$	0.65 ± 0.04	0.50 ± 0.03	0.15 ± 0.07
$Al_{1.0}CoCrCuFeNi$	0.65 ± 0.03	0.48 ± 0.03	0.17 ± 0.06
$Al_{2.0}CoCrCuFeNi$	0.70 ± 0.02	0.32 ± 0.01	0.30 ± 0.03

μ_p, peak coefficient of friction; μ_{ss}, the steady state coefficient of friction; $\Delta\mu = \mu_p - \mu_{ss}$.

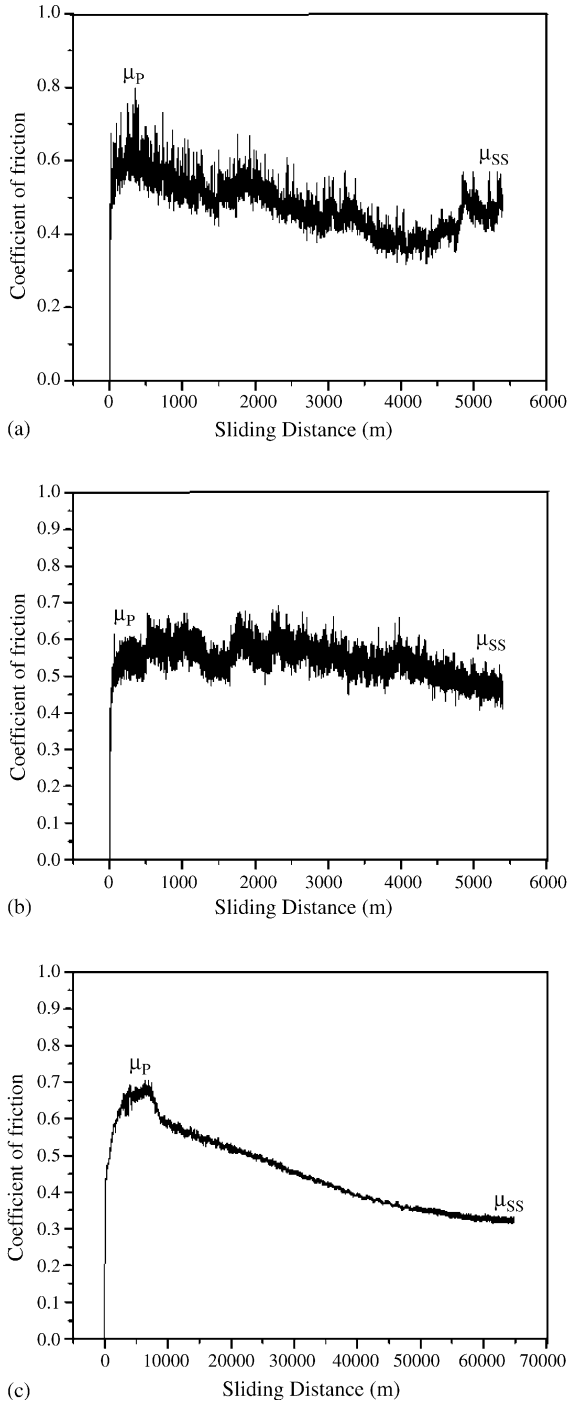

Fig. 8. Coefficient of friction vs. sliding distance curves, obtained using a normal load of 29.4 N and a sliding speed of 0.5 m/s under unlubricated sliding condition, for: (a) $Al_{0.5}CoCrCuFeNi$; (b) $Al_{1.0}CoCrCuFeNi$; (c) $Al_{2.0}CoCrCuFeNi$.

tion coefficient is due to the wear mechanism is of oxidation wear in contrast to the delamination wear. Fig. 8 also shows that $Al_{0.5}CoCrCuFeNi$ and $Al_{1.0}CoCrCuFeNi$ alloys exhibit relatively large fluctuation whereas $Al_{2.0}CoCrCuFeNi$ alloy does a small fluctuation. The large fluctuation of the friction coefficient is thought to be caused by two reasons. The first is the periodic localized fracture of surface layer [16]. The second is the periodic accumulation and elimination of debris on the worn surface. The coefficient of friction increases as the large-sized debris accumulates on the worn surface while it decreases as the debris depart from the worn surface. As for the small fluctuation of $Al_{2.0}CoCrCuFeNi$ alloy, it is due to its wear mechanism is of oxidative wear which results in small debris as mentioned in last section.

4. Conclusions

With increasing the aluminum content in the $Al_xCoCrCuFeNi$ alloys, both the volume fraction of strong BCC phase and the hardness value increase, nevertheless, the wear coefficient decreases and the wear mechanism changes from delamination wear to oxidative wear. For low aluminum content, $x = 0.5$, the microstructure is of simple ductile FCC phase and the worn surface is deeply grooved and undergoes a periodic delamination which produces big debris. For medium aluminum content, $x = 1.0$, the microstructure is a mixture of FCC and BCC phases, and the worn surface is deeply grooved in FCC region but smooth in BCC region. Delamination wear is still dominant although oxidative wear occurs in the smooth region. For high aluminum content, $x = 2.0$, the microstructure is of BCC phase and the worn surface is smooth and yields fine debris with high oxygen content. The high aluminum content gives a large improvement in wear resistance. This improvement is attributed to its high hardness, which not only resists plastic deformation and delamination, but also brings about the oxidative wear in which oxide film could assist the wear resistance.

Acknowledgements

The authors gratefully acknowledge the financial supports for this research by the National Science Council of Taiwan under grant no. NSC-91-2120-E-007-007 and the Ministry of Economic Affairs of Taiwan under grant no. 92-CE-17-A-08-S1-0003.

References

[1] J.W. Yeh, S.K. Chen, S.J. Lin, J.Y. Gan, T.S. Chin, T.T. Shun, C.H. Tsau, S.Y. Chang, Nanostructured high-entropy alloys with multiple principal elements: novel alloy design concepts and outcomes, Adv. Eng. Mater. 6 (2004) 299–303.
[2] S. Ranganathan, Alloyed pleasures: multimetallic cocktails, Curr. Sci. 85 (2003) 1404–1406.
[3] P.K. Huang, J.W. Yeh, T.T. Shun, S.K. Chen, Multi-principal-element alloys with improved oxidation and wear resistance for thermal spray coating, Adv. Eng. Mater. 6 (2004) 74–78.
[4] C.Y. Hsu, J.W. Yeh, S.K. Chen, T.T. Shun, Wear resistance and high-temperature compression strength of FCC $CuCoNiCrAl_{0.5}Fe$ alloy with boron addition, Metall. Mater. Trans. A 35A (2004) 1465–1469.
[5] C.J. Tong, Y.L. Chen, S.K. Chen, J.W. Yeh, T.T. Shun, C.H. Tsau, S.J. Lin, S.Y. Chang, Microstructure characterization of $Al_xCoCrCuFeNi$ high-entropy alloy system with multiprincipal elements, Metall. Mater. Trans. A 36 (2005) 881–893.
[6] C.J. Tong, M.R. Chen, S.K. Chen, J.W. Yeh, T.T. Shun, S.J. Lin, S.Y. Chang, Mechanical performance of the $Al_xCoCrCuFeNi$ high-entropy alloy system with multiprincipal elements, Metall. Mater. Trans. A 36A (2005) 1263–1271.

[7] P.J. Blau, Friction and Wear Transitions of Materials, Noyes Publishing, New Jersey, 1989.
[8] N.P. Suh, Tribophysics, Prentice-Hall, New Jersey, 1986.
[9] P.J. Blau, Model for run-in and other transitions in sliding friction, J. Tribol. 109 (1987) 537–544.
[10] D.A. Rigney, J.P. Hirth, Plastic deformation and sliding friction of metals, Wear 53 (1979) 345–370.
[11] D. Kuhlmann-Wilsdorf, Dislocation concepts in friction and wear, in: D.A. Rigney (Ed.), Fundamentals of Friction and Wear of Materials, ASM, Metals Park, Ohio, 1980, p. 119.
[12] N.P. Suh, Update on the delamination theory of wear, in: D.A. Rigney (Ed.), Fundamentals of Friction and Wear of Materials, ASM, Metals Park, Ohio, 1980, p. 43.
[13] Z.N. Farhat, Contribution of crystallographic texturing to the sliding friction behaviour of FCC and HCP metals, Wear 250 (2001) 401–408.
[14] J.P. Hirth, D.A. Rigney, The application of dislocation concepts in friction and wear, in: F.R. Nabarro (Ed.), Dislocations in Solids, vol. 6, North-Holland, Amsterdam, 1983, p. 10.
[15] R.E. Reed-Hill, R. Abbaschian, Physical Metallurgy Principles, third ed., PWS-KENT Publishing Company, Boston, 1994, pp. 140–146.
[16] T. Courtney, Mechanical Behavior of Materials, McGraw-Hill, New York, 1990, pp. 173–184.
[17] G.E. Dieter, Mechanical Metallurgy, SI Meric ed., McGraw-Hill Book Company, New York, 1988, pp. 117–121.
[18] G.E. Dieter, Mechanical Metallurgy, SI Meric ed., McGraw-Hill Book Company, New York, 1988, pp. 208–212.
[19] M.M. Khruschov, Principles of abrasive wear, Wear 28 (1974) 69–88.
[20] Y. Wang, T.Q. Lei, J.J. Liu, Tribo-metallographic behavior of high carbon steels in dry sliding. I. Wear mechanisms and their transition, Wear 231 (1999) 1–11.